Utilizing Minutia Density Distribution and the Desmos Service for Fingerprint Wrinkle Detection

Firas S. Abdulameer

Department of physics
College of Science, Mustansiriyah University Baghdad, Iraq
firasalaraji@uomustansiriyah.edu.iq

ABSTRACT

Fingerprint recognition is one of the safe methods that may be utilized to identify individuals automatically. It has garnered a lot of interest and is being used extensively in a variety of civilian applications, such as finance and access control, amongst other things. One of the primary components in image processing applications is a fingerprint, which refers to human attributes used for user authentication. Wrinkles destroy the structure and texture of a fingerprint, notably by severing ridgelines and creating a sequence of spurious minutiae. The presence of wrinkles is fatal to the structure and texture of a fingerprint. Therefore, creases make fingerprint recognition methods less accurate, particularly the method that is now considered the most reliable based on minutiae matching. In this paper, we investigate the detection of wrinkles from fingerprint images, including two aspects that handle wrinkles and reconstruct ridges. First, the distance between pseudo-minutiae pairings is calculated. Then, shelves are rebuilt utilizing Newton polynomial interpolation and the online service desmos. In the paper, results are presented.

Keywords: Fingerprint recognition; Newton polynomial interpolation; Wrinkles detection; Wrinkles repair; Minutia density.

I. INTRODUCTION

Fingerprint-based identification is becoming more common as the need for automated person-identifying technology grows. When compared to other forms of biometric information, such as the face, speech, iris, and gesture, the fingerprint provides the most reliable evidence for labeling. Extraction of features, gathering of data, and matching are the three fundamental processes that make up a general fingerprint identification system [1]. For the stage of fingerprint matching, fingerprints are generally defined by two-minute minutiae, such as the end and bifurcation of ridges. This is because fingerprints are resilient to numerous types of fingerprint degeneration. For example, the ANSI-NIST regular fingerprint description is based on minutiae [2]. Because ridge orientation is inextricably linked to matching, describing, and detecting minutiae, proper image segmentation aids in avoiding the detection of artificial minutiae in low-quality image areas In addition, the estimation of ridge orientation and the segmentation of images are extremely important components of the minutiae detection and matching process [2, 3].

After a fingerprint has been subjected to various preprocessing techniques, such as binarization, enhancement, thinning, and so on, the primary objective of the minutia-extraction technique is to acquire the minutiae from the fingerprint. The matching step, as its name suggests, involves determining whether or not two fingerprints come from the same finger by evaluating the degree to which they resemble one another and making a determination based on that comparison. It is relevant for performance enhancement in a minutiae-based recognition system to have accurate minutiae retrieval with more minor omissions or erroneous extraction processes.

Recent suggestions for estimating the orientation field (OF) of fingerprint patterns have included gradient schemes, strategies based on slits and projections, techniques that focus on grey-level consistency and variation, and frequency-area calculations [4, 5]. Gradient squared averaging is the most common method for determining the orientation field of an image block [6-9] due to its superior performance and resolution. This is one of the factors for its effectiveness. Since gradient extraction may be affected by noise and other defects, the orientation map (OM) estimation [10] may not be precise. On the other hand, an orientation smoothing stage can alleviate this difficulty and provide a improved illustration of the ridge construction for fingerprint categorization. The precision of the recognition of fingerprints algorithm is significantly affected by the quality of the fingerprint photographs. Because some of the fingerprint photos aren't very good, the minutiae are going to be extracted improperly, which will lead to mistake matching. Creases characterized by collinear terminations on ridges [4] are one of the unfortunate images. It can, fortunately, repair creases. Based on the research conducted by Jian et al. [3] and Zhou J et al. [10, 11], fingerprint recognition for elderly individuals frequently includes wrinkles. However, even when fingerprint images are charged from Younger individuals, they are immediately obscured by creases caused by the sensor's precision, skin dryness, incisions, dirt, and oil stain. Gottschlich et al. [14] presented an original method for estimating the frequency of occurrence that was based on retracing ridge and valley lines. This approach is unaffected by disturbances such as scars, moisture, pollution, or dryness of the fingers, for example. Comparisons are made between a gradient-based approach, a multiscale directional operator, and the line-sensor method in order to determine which method produces the best results when compared to the others. Experiments with simulated scar noise are used to test its robustness. These experiments are performed on top of high-quality fingerprint photos taken from the FVC2000 and FVC2002 databases. Last but not least, using 60 fingerprint photographs from the FVC2004 database that are, for the most part, of mediocre quality, the efficiency of the line-sensor-based technique that was utilized for showing this technique was demonstrated. Wu et al. [10] considered a new fingerprint pattern termed crease, a series of uneven stripes that cross the typical fingerprint patterns (valleys and ridges). By employing traditional feature detection methods, wrinkles will produce spurious minutiae, lowering the acceptance rate of fingerprint classification. By defining the crease using a parameterized rectangle, In order to recognize creases in a number of different directions, the author develops a superior detector and makes use of a multi-channel filtering architecture. Each channel uses PCA to calculate rectangle parameters from raw detected data. Using the minutia density distribution, Jian et al. [3] provided a new crease identification and rectification method. Creases are isolated from others using the minutia density distribution and then divided into SODCAs and LODCAs. The distribution of the orientation field is known to alter greatly in two different types of crease areas, and the pseudo minutiae pairings are notoriously difficult to unify. For minutiae pairing, we use Least Deviation, and for reconnections, we use stepwise approximate. The triangle constraint approach and the standard calibration methodology are better suitable in LODCAs. With further calculations, the program can detect and correct wrinkles. Chauhan et al. [15] investigated wrinkle properties for fingerprint categorization. The public Hong Kong PolyU high-resolution fingerprint data DBII was tested. The experiments reveal that creases can greatly improve fingerprint matching. Chen et al. [16] introduced a minutiae-based fingerprint identification technique. In the matching stage, the orientation field of a fingerprint is reconstructed from its minutiae in order to increase processing speed. After performing interpolation in the sparse area, an orientation model will recreate the perspective field using "virtual" and "real" minutiae as building blocks. Decision fusion integrates minutiae-based and reconstruction orientation field comparison. Since fingerprint orientation fields are global properties, the suggested

method can produce more accurate results than current methods.

In order to enhance the recognition accuracy of low-quality fingerprint images, crease detection and repair must be performed. The creases will divide the normal ridgelines, resulting in a number of pseudo-details in these regions. As a consequence of this, we provide a technique for identifying creases that is predicated on the distribution of the Minutia Density (MD). To begin, determine the amount of space that separates each pair of pseudo minutiae. The second step is to recreate the ridges by utilizing the Newton Polynomial Interpolation method and the website desmos.com. The findings suggest that there was a discernible improvement in recognition accuracy after the wrinkles were repaired.

The remaining sections of the paper are organized as follows: The intent is to develop a wrinkle detection and restore ridges algorithm using the method described in Section 2. Sections 3 and 4 contain the respective results and conclusions.

II. Detection and Reconstruction Wrinkle for Fingerprint Images

Many people have worked on fingerprint ridge orientation, resulting in gradient [18-20], orientation field modelling [4, 21, 22], neural network [23, 24], and ridge projection methods [25, 26]. Gradient methods [18-20] and orientation field modelling [4, 21, 22] are examples.

2.1 Wrinkle Detection

Some erroneous or deleted minutiae will significantly reduce the precision of a method that relies on minutiae. The folds will penetrate traditional ridges and introduce an abundance of fictitious details. Two or more endpoints are produced on opposing sides of the crease as a consequence of the ridge-cutting action of the crease. The frequent lack of contrast in wrinkle regions complicates matters. It is challenging to differentiate the summits from the background and the valleys. As shown in Figure 1, some initially parallel ridges may intersect in fissure regions, producing pseudo bifurcates or even pseudo single points. (c). In conclusion, fissures alter local structure, introduce spurious information, and distort larger configurations, such as orientation and frequency area distribution. It is crucial to have precise connections between pseudo-details and fewer incorrect connections between distinct creases and typical ridges. By reestablishing these connections, the impact on the original biometric infrastructure will be reduced. According to Zhou J. et al. [11], wrinkles maintain their form over an extended period of time, which enables them to function as separate features and crucial fingerprint identifying features. It is essential to identify and categorize creases in the beginning. The MD is defined as the total amount of minutiae in a specified area following minutia extraction. The distribution of minute details is widespread and the MD values are comparatively small. In wrinkle zones, the pseudo minutiae result in a significantly increased MD. At the moment, we can identify significant MD areas as potential crease candidates. We create a fixed-size $G * K$ orthogonal box depending on the distribution of orientation fields surrounding the destination (see Fig. 2). The edge G represents a field with a vertical orientation. The orientation field runs parallel to the edge in a perpendicular direction K.

(a) (b)

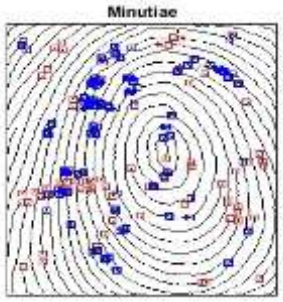

(c)

Figure 1. (a) Unique image. (b) Image thinning. (c) The fingerprint minutiae extracted

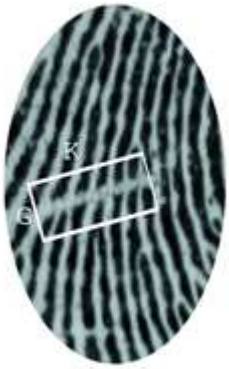

Figure 2. *The MD calculation diagram*

The breadth and length of the wrinkle are connected to the $G\,K$ values. Variations in the crease and common regions will be blurred if the values are too little or too large. If the MD value at point (x, y) is behind $\mathrm{TH_{md}}$, then the point refers to the wrinkle candidate region.

$$TH_{md} = num/(G.K) \quad (1)$$

Some constraints were placed on the crease model by Zhou et al. [11] and Jian et al. [3], as shown in the following:

$$w > TH1,\ l > TH2, and\ l/w > TH3 \quad (2)$$

$$avg\{L(Cx, Cy, l, \emptyset)\} > TH4 \quad (3)$$

$$\emptyset > TH5 \quad (4)$$

Where $L(Cx, Cy, l, \emptyset)$ denotes the wrinkle curve, (Cx, Cy), w, l and $\emptyset$ are the coordinates of the center points, breadth, length of sentence, and wrinkle orientation L for each wrinkle individually. Each avg $\{L(Cx, Cy, l, \emptyset)\}$ represents the grayscale that is typical for the wrinkle L. $\emptyset$ is the difference in the orientation of the wrinkle curvature compared to the normal ridges. TH5, TH4,TH3,TH2, and TH1 are all preliminary values. Figure 3 illustrates the schematic explanation of the wrinkle detection process.

(a) (b)

Figure 3. (a) Image of the objective fingerprint, (b) The image's large MD sections are denoted by blue bars.

2.2 Repair and Reconstruct of Wrinkles

In this section, we handle the wrinkles and build ridges of a fingerprint. The purpose here is two-fold: determine the distance among two pairing of pseudo minutiae and recreate ridges using the Newton polynomial interpolation. We introduce our technique in two main steps:

Step 1: Minutiae Pairing Pseudo

Fig.5 exhibits pseudo minutiae are approximately similar. There are eight pseudo minutiae in this zone, labelled as A_1 -A_4 and a_1 - a_4, separately.

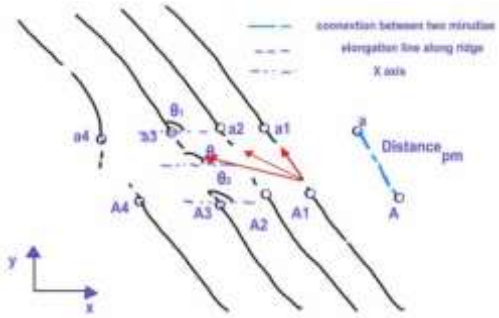

Figure 4. Diagram of eight ridge minutiae

There are four essential parameters for each pairing sample: couple adjustment values of the minutiae pairing, $\emptyset_1$ and $\emptyset_2$, distance

Distance $_{pm}$ among them, and the angle $\emptyset$ between the x-axis and two-point connection. As we mentioned above, the pseudo minutiae are almost comparable; based on this assumption, the angle is $\emptyset$ constant, i.e., the orientation values, $\emptyset_1$ and $\emptyset_2$ are constant. Using the following equation, we may determine the distance that exists between two partnering endpoints of pseudo-microscopic organisms.

$$\text{Distance}_{pm} = \sum_{k=1}^{M}\sum_{z=1}^{N}\sqrt{(A_k - a_z)^2} \quad (5)$$

Where Distance_{pm} the area separating the two paired ends of pseudo minutiae is, $A = \{A_1, A_2, A_3, ..., A_k\}$ $a = \{a_1, a_2, a_3, ..., a_z\}$ is an individual instance of both the set of an end ridge and the set of an opposing ridge. If Equation (5) is correct, then we should have stacks, which are defined in the following way

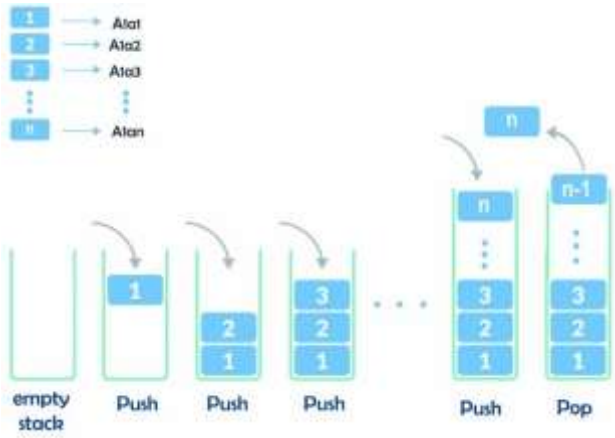

Figure 5. Stacks diagram

Subsequently, we pick the most insignificant number that still fits the limitations of Equation (5), and after that, we can obtain $A_1 - a_1, A_2 - a_2, A_3 - a_3$, and $A_4 - a_4$ minutiae pairs. The distance that separates any two ridgelines can range anywhere from 5 to 23 pixels [11-14]. In Figure 6, the line with dots represents the extension line of the ridgeline along the direction, whereas the line with solids represents the traditional line of the mountainside at point A_2. Points A_3 and A_2 are located on opposing sides of the central line, although at point Q, the normal line creates a ridgeline in the landscape. On the same ridgeline as Point Q and A_3. It is possible to determine that locations C and A are located on the same side of the standard line if the Euclidean distance between them is less than 23 pixels. Points a_2, a_1, and a_3 are the ones who are still in the running. They are all situated on the opposing side of A_2. The point that is estimated to be the furthest away is eliminated from consideration for A's partnering point. Similarly, $A_1. - a_1$ and $A_3. - a_3$ pairs can be found.

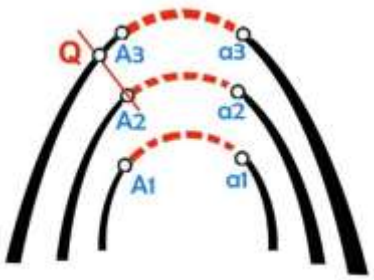

Figure 6. Fingerprint and minutiae distribution diagram

Step 2: Pseudo Minutiae Pair reconstruction

After pairing, newton polynomial interpolation and application of the online service desmos.com [27] are achieved for reconnecting paired minutiae. Our steps are explained below:

1- Thinning type of fingerprint image must be used.
2- Image Insertion to the application of online service desmos.com, which draws a curve by connecting between minutiae pairing that select in step 1 as shown in Fig. 7.

Figure 7. Image application in desmos

3- Five points should be selected, including end minutiae pairing on the curve, to

extract the values (x, y) between minutiae pairing, as shown in Fig. 8 and Table 1.

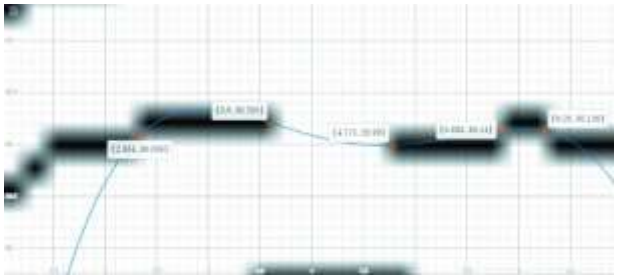

Figure 8. Five points on the curve in desmos

TABLE 1. THE FIVE POINTS IN DESMOS

x	f(x)
2.334	30.083
3.6	30.205
4.775	29.99
5.835	30.14
6.25	30.126

4- Following that, in order to determine the x value of the subsequent point, we select a point on the curve depicted in Figure 9 that lies between the two minutiae points.

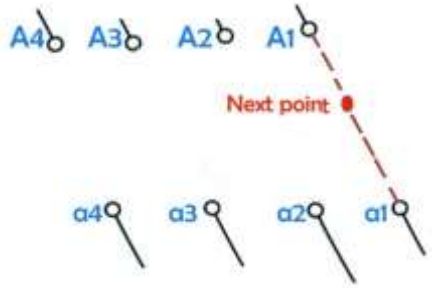

Figure 9. Determine the next minutiae point

5- Finally, applying value (x) that extract in the above step in Newton interpolating polynomials (NIP) method based on the following equation to get the y value of the next minutiae points.

$$f(x) = b_0 + b_1(x-x_0) + b_2(x-x_0)(x-x_1) + \ldots + b_n(x-x_0)(x-x_1)\ldots\ldots(x-x_{n-1}) \quad (6)$$

Previously we get into calculating the coefficients, it's worth noting that Equation (6) is an *nth* order polynomial, as demonstrated by the past term, which contains the necessary power of x, specifically x^n All powers of x are existing in Equation (6) even though the coefficients of say $y_0 = f(x_0)$ and $y_1 = f(x_1)$ etc. Since there are $n+1$ independent coefficients bi available, $i = 0, 1, 2, \ldots, n$, we can be confident that at most an nth order polynomial passes within the information points presented. After looking at a few simple instances, the justification for using the analytical form in Equation (6) will become clear.

Set $(x_0, y_0), (x_1, y_1)$ where $y_0 = f(x_0)$ and $y_1 = f(x_1)$

When $n = 1$ and there are two data points, the first order polynomial is

$$f_1(x) = b_0 + b_1(x\text{-}x_0) \quad (7)$$

Replacement of the double data points $(x_0, y_0), (x_1, y_1)$ into Equation (7) provides

$$f_1(x_0) = b_0 + b_1(x_0\text{-}x_0) \quad (8)$$

$$f_1(x_1) = b_0 + b_1(x_1\text{-}x_0) \quad (8a)$$

Solving for $b0$ and $b1$ yields,

$$b_0 = f_1(x_0) \quad (9)$$

$$b_1 = \frac{f_1(x_1) - f_1(x_0)}{x_1 - x_0} \quad (9a)$$

By scheme, the actual function $f(x)$ and the interpolating function $f_1(x)$ which the data points were obtained are equivalent to one another at $x = x_0$ and $x = x_1$. As a result, b_1

and b_0 can be shown in terms of the given data,

$$b_0 = f(x_0) \qquad (10)$$

$$b_1 = \frac{f(x_1) - f(x_0)}{x_1 - x_0} \qquad (10a)$$

Lastly, comparing the y value of the next minutiae point in desmos application and the y value of the next minutiae point that we calculated using NIP are equal. This indicates the correctness of our method.

III. Results

In this part, the database includes different finger images, and all the processes are implemented and evaluated on desmos and Matlab. The findings indicate that the strategy has the potential to enhance the reconstruction

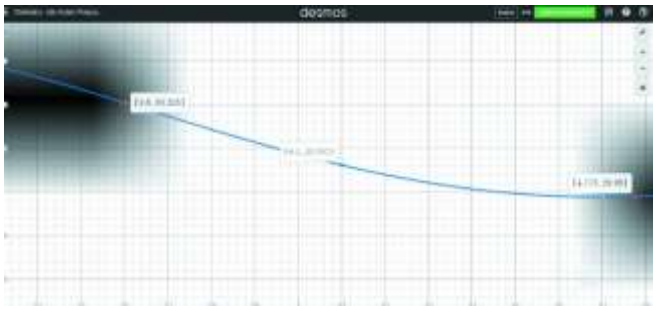

of fingerprint creases by pinpointing the subsequent site of minutiae matching. In actual use, our approach performs more admirably than that of our competitors (see Fig 10).

Figure 10. Reconstruct the next point of minutiae pairing

IV. Conclusion

This research work investigated the detection of creases in fingerprint photographs. Additionally, we improved the performance of wrinkle detection within the fingerprint recognition system, incorporating both of its features. First, we determined the gap in distance between each pair of pseudo minutiae using the appropriate formula. Second, we recreated ridges by applying the NIP and calculating the next point of minutiae pairing to do so. This was done by using the desmos application. The findings suggest that increased performance in fingerprint recognition can be achieved by rebuilding ridges from generated minutiae. In upcoming work, our primary focus will be developing new ways to combine existing methods to improve wrinkles detection performance.

References

[1] M. NarayanMohanty and R. Sikka, "oReview on fingerprint-based identification system," Materials Today: Proceedings, 2021.

[2] L. N. Darlow and B. Rosman, "Fingerprint minutiae extraction using deep learning," in 2017 IEEE International Joint Conference on Biometrics (IJCB), 2017, pp. 22-30: IEEE.

[3] W. Jian, Y. Zhou, H. Liu, and N. Zhu, "Crease Detection and Repair Based on Minutia Density Distribution," in 2019 IEEE 11th International Conference on Communication Software and Networks (ICCSN), 2019, pp. 446-451: IEEE.

[4] W. Bian, D. Xu, Q. Li, Y. Cheng, B. Jie, and X. Ding, "A survey of the methods on fingerprint orientation field estimation," IEEE Access, vol. 7, pp. 32644-32663, 2019.

[5] R. Gupta, M. Khari, D. Gupta, and R. G. Crespo, "Fingerprint image enhancement and reconstruction using the orientation and phase reconstruction," Information Sciences, vol. 530, pp. 201-218, 2020.

[6] A. A. ABBOOD, G. SULONG, A. M. TAHA, and S. U. PETERS, "A new technique for estimating and enhancing orientation field of fingerprint image," Journal of Theoretical and Applied Information Technology, vol. 96, no. 7, 2018.

[7] C. Yuan and X. Sun, "Fingerprint liveness detection using histogram of oriented gradient based texture feature," Journal of Internet Technology, vol. 19, no. 5, pp. 1499-1507, 2018.

[8] E. P. Wibowo, S. A. Harseno, and R. K. Harahap, "Feature Extraction Using Histogram of Oriented Gradient and Hu Invariant Moment for Face Recognition," in 2018 Third International Conference on Informatics and Computing (ICIC), 2018, pp. 1-5: IEEE.

[9] D. Zabala-Blanco, M. Mora, R. J. Barrientos, R. Hernández-García, and J. Naranjo-Torres, "Fingerprint Classification through Standard and Weighted Extreme Learning Machines," Applied Sciences, vol. 10, no. 12, p. 4125, 2020.

[10] C. Wu, J. Zhou, Z.-q. Bian, and G. Rong, "Robust crease detection in fingerprint images," in 2003 IEEE Computer Society Conference on Computer Vision and Pattern Recognition, 2003. Proceedings., 2003, vol. 2, pp. II-505: IEEE.

[11] J. Zhou, F. Chen, N. Wu, and C. Wu, "Crease detection from fingerprint images and its applications in elderly people," Pattern Recognition, vol. 42, no. 5, pp. 896-906, 2009.

[12] M. Sarfraz, "Introductory Chapter: On Fingerprint Recognition," in Biometric Systems: IntechOpen, 2021

[13] J. M. Singh, A. Madhun, G. Li, and R. Ramachandra, "A survey on unknown presentation attack detection for fingerprint," arXiv preprint arXiv:2005.08337, 2020.

[14] C. Gottschlich, P. Mihailescu, and A. Munk, "Robust orientation field estimation and extrapolation using semilocal line sensors," IEEE Transactions on Information Forensics and Security, vol. 4, no. 4, pp. 802-811, 2009.

[15] N. Chauhan, M. Soni, V. Anand, and V. Kanhangad, "Fingerprint classification using crease features," in 2016 IEEE Students' Technology Symposium (TechSym), 2016, pp. 56-60: IEEE.

[16] F. Chen, J. Zhou, and C. Yang, "Reconstructing orientation field from fingerprint minutiae to improve minutiae-matching accuracy," IEEE Transactions on image processing, vol. 18, no. 7, pp. 1665-1670, 2009.

[17] [17] W. Bian, Y. Luo, D. Xu, and Q. Yu, "Fingerprint ridge orientation field reconstruction using the best quadratic approximation by orthogonal polynomials in two discrete variables," Pattern recognition, vol. 47, no. 10, pp. 3304-3313, 2014.

[18] Y. Wang, J. Hu, and F. Han, "Enhanced gradient-based algorithm for the estimation of fingerprint orientation fields," Applied Mathematics and Computation, vol. 185, no. 2, pp. 823-833, 2007.

[19] C. Gottschlich, E. Marasco, A. Y. Yang, and B. Cukic, "Fingerprint liveness detection based on histograms of invariant gradients," in IEEE international joint conference on biometrics, 2014, pp. 1-7: IEEE.

[20] L. Wieclaw, "Gradient based fingerprint orientation field estimation," Journal of Medical Informatics & Technologies, vol. 22, 2013.

[21] D. Chen, X. Ji, F. Fan, J. Zhang, L. Guo, and W. Meng, "Comparative analysis of fingerprint orientation field algorithms," in 2009 Fifth International Conference on Image and Graphics, 2009, pp. 796-801: IEEE.

[22] S. Jirachaweng, Z. Hou, J. Li, W.-Y. Yau, and V. Areekul, "Residual Analysis for Fingerprint Orientation Modeling," in 2010 20th International Conference on Pattern Recognition, 2010, pp. 1196-1199: IEEE.

[23] D. T. Meva, C. Kumbharana, and A. D. Kothari, "The study of adoption of neural network approach in fingerprint recognition," International Journal of Computer Applications, vol. 40, no. 11, pp. 8-11, 2012.

[24] H. Fan, P. Su, J. Huang, P. Liu, and H. Lu, "Multi-band MR fingerprinting (MRF) ASL imaging using artificial-neural-network trained with high-fidelity experimental data," Magnetic resonance in medicine, 2021.

[25] E. Jarocka, J. A. Pruszynski, and R. S. Johansson, "Human touch receptors are sensitive to spatial details on the scale of single fingerprint ridges," Journal of Neuroscience, vol. 41, no. 16, pp. 3622-3634, 2021.

[26] J. Priesnitz, C. Rathgeb, N. Buchmann, C. Busch, and M. Margraf, "An overview of touchless 2D fingerprint recognition," EURASIP Journal on Image and Video Processing, vol. 2021, no. 1, pp. 1-28, 2021.

[27] https://www.desmos.com/ (the date of access: 21.02.2021).